USE OF SOMMERFELD'S THEORY FOR THE CALCULATION OF THE CURRENT DISTRIBUTION ON PRINTED BOARDS BASED ON NEARFIELD MEASUREMENTS

G. Fässler and F. M. Landstorfer
Institut für Hochfrequenztechnik, Universität Stuttgart
Pfaffenwaldring 47, 70550 Stuttgart, Germany

1. Introduction

A method for measuring the currents on a printed circuit board has been developed. The magnetic field strength above the board is scanned by small probes and used to calculate the currents that cause these fields. The numerical backtransformation is based on the Method of Moments and uses Sommerfeld's theory for stratified media to represent the substrate of the printed board and an infinite ground plane. This inverse problem is inherently ill-posed and leads to an ill-conditioned system of linear equations which is solved by the conjugate gradient method, taking advantage of the regularizing properties of this method.

Results are given for a branch line coupler at 2.25GHz on a RT-duroid substrate in microstrip technique.

2. Circuit Board Model and Measurement Setup

Figure 1 shows the model of the circuit board used for the calculations. The board is modelled by a wire grid with a constant filament current in each segment. Entire domain basis functions as well as triangular basis function were tested but resulted in a poorer performance when measurement error was present [1]. The substrate and the ground plane are considered by a special Green's function and need not be modelled separately. Due to the constant current distribution the charges are concentrated at the knots of the grid and can be evaluated by the equation of continuity

$$\underline{Q}_{\mu\nu} = \frac{1}{j\omega}\left(\underline{I}_{x,\mu-1,\nu} - \underline{I}_{x\mu\nu} + \underline{I}_{y,\mu,\nu-1} - \underline{I}_{y\mu\nu}\right). \tag{1}$$

At the edge of the grid the number of terms is reduced respectively.

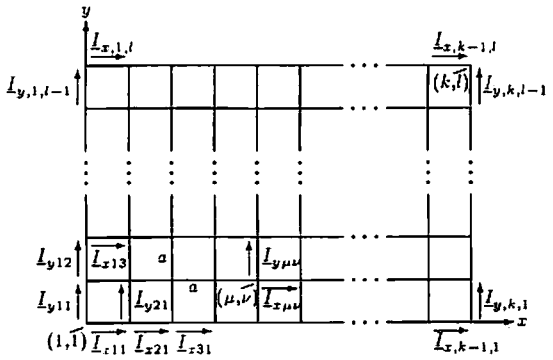

Figure 1: Model of the circuit board

Measurements of the magnetic fields $\underline{H}_x$ and $\underline{H}_y$ are taken at a constant height z_0 above the knots of the grid. They are assigned the indices μ and ν of the corresponding points. For the backtransformation no information about the electric field components is necessary but can be used to improve the result.

Using Maxwell's equations in their time-harmonic form gives a relation between the currents and the magnetic fields:

$$\underline{H}_x(\tilde{x},\tilde{y},\tilde{z}_0) = \sum_{\mu=1}^{k-1}\sum_{\nu=1}^{l} \underline{f}_x(\tilde{x}-\mu,\tilde{y}-\nu,\tilde{z}_0)\cdot\underline{I}_{x\mu\nu} + \sum_{\mu=1}^{k}\sum_{\nu=1}^{l-1} -\underline{f}_y(\tilde{y}-\nu,\tilde{x}-\mu,\tilde{z}_0)\cdot\underline{I}_{y\mu\nu} \tag{2}$$

$$\underline{H}_y(\tilde{x},\tilde{y}.\tilde{z}_0) = \sum_{\mu=1}^{k-1}\sum_{\nu=1}^{l}\underline{f}_y(\tilde{x}-\mu,\tilde{y}-\nu,\tilde{z}_0)\cdot\underline{I}_{x\mu\nu} + \sum_{\mu=1}^{k}\sum_{\nu=1}^{l-1}\underline{f}_x(\tilde{y}-\nu,\tilde{x}-\mu,\tilde{z}_0)\cdot\underline{I}_{y\mu\nu} \quad (3)$$

$$(\tilde{x}=1,2,3,\ldots,k \qquad \tilde{y}=1,2,3,\ldots,l)$$

Here the tilde indicates that all values are normalized with respect to a, the grid constant.

3. Computation of the Green's Function

The functions $\underline{f}_x$ and $\underline{f}_y$ depend only on the geometry of the structure and contain the Green's function of the specific substrate. For the calculation an x-directed horizontal electric dipole of moment Idx is placed in the air-dielectric interface of a microstrip structure with infinite transverse directions as shown in figure (2).

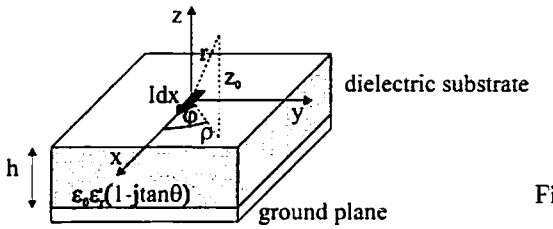

Figure 2: Geometry for the horizontal electric dipole

The origin of the coordinate system is at the location of the dipole and the ground plane is at height $z=-h$. The configuration is transformed to the spectral domain by a Hankel transformation replacing the distance ρ by the radial wave number k_ρ. For a stratified medium it is possible to use $\underline{E}_z$ and $\underline{H}_z$ as potentials [2] and the remaining transverse field components can be evaluated by:

$$k_\rho^2\underline{E}_x = -jk_x\dot{\underline{E}}_z - \omega\mu k_y\underline{H}_z \quad (4) \qquad k_\rho^2\underline{H}_x = -jk_x\dot{\underline{H}}_z + \omega\epsilon k_y\underline{E}_z \quad (6)$$

$$k_\rho^2\underline{E}_y = -jk_y\dot{\underline{E}}_z + \omega\mu k_x\underline{H}_z \quad (5) \qquad k_\rho^2\underline{H}_y = -jk_y\dot{\underline{H}}_z - \omega\epsilon k_x\underline{E}_z \quad (7)$$

with $\underline{k}^2=\omega^2\underline{\epsilon}\mu=k_x^2+k_y^2+\underline{k}_z{}^2=k_\rho^2+\underline{k}_z{}^2$, $\dot{\underline{H}}_z=\frac{\partial\underline{H}_z}{\partial z}$ and $\dot{\underline{E}}_z=\frac{\partial\underline{E}_z}{\partial z}$.

The solution for the potentials $\underline{E}_z$ and $\underline{H}_z$ can be derived by applying the boundary conditions for the tangential and the normal fields at the air-dielectric interface and at the perfectly conducting ground plane. These conditions are satisfied if $\underline{H}_z$ and $\dot{\underline{E}}_z$ are continuous at the air-dielectric interface and $\underline{H}_z$ and $\dot{\underline{E}}_z$ becomes 0 at the ground plane. $\underline{\epsilon}\,\underline{E}_z$ and $\dot{\underline{H}}_z$ jump according to the dipole moment $g_x=e_x\frac{\delta(\rho)}{2\pi\rho}Idx$ and the associated charges. In spectral domain the solutions for the potentials are given by ($z_0>=$):

$$2\pi j\omega\epsilon_0\underline{E}_z(k_x,k_y.z_0) = -jk_xIdx\frac{\underline{u}_1\tanh\underline{u}_1h}{\epsilon_r\underline{u}_0+\underline{u}_1\tanh\underline{u}_1h}e^{-\underline{u}_0z_0} \quad (8)$$

$$2\pi\underline{H}_z(k_x,k_y.z_0) = -jk_yIdx\frac{1}{\underline{u}_0+\underline{u}_1\coth\underline{u}_1h}e^{-\underline{u}_0z_0} \quad (9)$$

with $\underline{u}_0{}^2=k_\rho^2-k^2$ and $\underline{u}_1{}^2=k_\rho^2-\underline{\epsilon}_rk^2$.

Using the equations (6) and (7) and transforming the solution to the space domain gives the result for the two requested magnetic fields:

$$\underline{H}_x(\rho,\varphi,z_0) = \frac{Idx}{2\pi}(\underline{\epsilon}_r-1)\sin2\varphi\int_0^\infty\frac{k_\rho^3}{\underline{D}_E\underline{D}_H}e^{-\underline{u}_0z_0}\left(J_0(k_\rho\rho)-\frac{J_1(k_\rho\rho)}{2k_\rho\rho}\right)dk_\rho \quad (10)$$

$$\underline{H}_y(\rho,\varphi,z_0) = \frac{Idx}{2\pi}(\underline{\epsilon}_r-1)\int_0^\infty\frac{k_\rho^3}{\underline{D}_E\underline{D}_H}e^{-\underline{u}_0z_0}\left(\cos^2\varphi\,J_0(k_\rho\rho)-\cos2\varphi\frac{J_1(k_\rho\rho)}{k_\rho\rho}\right)dk_\rho$$
$$-\frac{Idx}{2\pi}\int_0^\infty J_0(k_\rho\rho)\frac{k_\rho\underline{u}_0}{\underline{D}_H}e^{-\underline{u}_0z_0}dk_\rho \quad (11)$$

The functions $\underline{D}_E$ and $\underline{D}_H$ are defined by $\underline{D}_E=\underline{\epsilon}_r\underline{u}_0+\underline{u}_1\tanh\underline{u}_1h$ and $\underline{D}_H=\underline{u}_0+\underline{u}_1\coth\underline{u}_1h$.

Similar results are obtained in [3] for the fields on the surface of a microstrip structure.

The solutions for $\underline{H}_x$ and $\underline{H}_y$ are used to define the functions $\underline{f}_x$ and $\underline{f}_y$ respectively by an integration over the fields of the dipole moment Idx along a segment.

4. Ill-Posed Problems and the L-Curve

Equations (2) and (3) are discrete 2-dimensional versions of Fredholm integral equations of the first kind. The general form of these equations is given by

$$\int_{t_1}^{t_2} \underline{x}(t)\underline{A}(s,t)\,dt = \underline{b}(s) \qquad s_1 \le s \le s_2, \tag{12}$$

where $\underline{A}$ (the kernel) and $\underline{b}$ (the right hand side) are known and $\underline{x}$ is a function to be evaluated. This kind of equation belongs to the group of ill-posed problems because small variations of the right hand side, which in general represents measured values, may cause rather large changes in the solution $\underline{x}$. In the discrete case, an ill-posed problem often results in an ill-conditioned system of linear equations.

In order to obtain meaningful solutions of such a problem, even when the right hand side contains measurement errors, regularization has generally to be used. Here the solution $\vec{\underline{x}}$ of the system of linear equations $\underline{\mathbf{A}}\,\vec{\underline{x}} = \vec{\underline{b}}$ is no longer given by solving the problem

$$\min \|\underline{\mathbf{A}}\,\vec{\underline{x}} - \vec{\underline{b}}\| \tag{13}$$

but by finding

$$\min \left\{ \|\underline{\mathbf{A}}\,\vec{\underline{x}} - \vec{\underline{b}}\|^2 + \lambda^2 \|\underline{\mathbf{L}}(\vec{\underline{x}} - \vec{\underline{x}}_0)\|^2 \right\}. \tag{14}$$

Here $\vec{\underline{x}}_0$ is an estimated solution, $\vec{\underline{x}}_0 = 0$ if no information is available, and $\underline{\mathbf{L}}$ is a suitably chosen matrix, generally either the identity matrix or a discrete approximation of a differential operator. λ is called the regularization parameter, it determines the relative weight of the second term in (14), which is a measure of the "smoothness" of the solution, with respect to the first term, the square norm of the residual.

Finding the right value of the regularization parameter is crucial for obtaining a good regularized solution to a problem. It is often chosen as a function of the estimated measurement errors. An interesting method for the case where no information about the error is available has been proposed by P. C. Hansen [5]. It consists in solving (14) for different values of the regularization parameter and plotting the "smoothness" measure $\|\underline{\mathbf{L}}\,(\vec{\underline{x}} - \vec{\underline{x}}_0)\|$ against the residual norm $\|\underline{\mathbf{A}}\,\vec{\underline{x}} - \vec{\underline{b}}\|$ in log-log scale. This curve, which is presented in figure 3, is called L-curve because it exhibits a characteristic bend. It can be shown [5] that this bend represents an optimal compromise between the two terms in (14) and that the corresponding value of λ is the optimal choice for the regularization parameter of this problem.

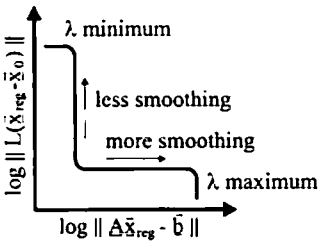

Figure 3: L-curve

The conjugate gradient method, which is used to solve the equation system, gives a regularized solution and the number of iteration steps k plays the role of the regularization parameter [4]. As the norm of the residual decreases for growing k, high values of k correspond to low values of λ in (14) and vice versa. The L-curve can be examined during the iteration and the algorithm can be stopped when the bend in the L-curve is reached.

5. Results

In order to verify the developed algorithm, the magnetic fields above the branch line coupler depicted in figure 6 were determined ($z_0 = 5$mm) and backtransformed. The board was modelled

with 15×10 knots and the distance between two knots was $a = 4.5$mm. Figure 4 shows the magnitude of the horizontal magnetic fields and figure 5 the computed current distribution. The input signal was applied to Port A with $P = 10dBm$ corresponding to 7.07mA. Details of the current along the upper conductor between Port C and D are given in figure 7. The directivity to Port C is approximately $40dB$ at the given frequency and the coupling attenuation is $3dB$.

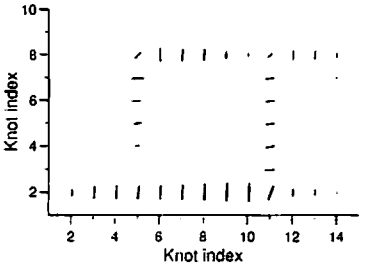

Figure 4: Field distribution of the tangential magnetic field 5mm above the board. Size and orientation of the symbols corresponds to the magnitude and the direction of the nearly linear polarized fields. Phase information is not visible.

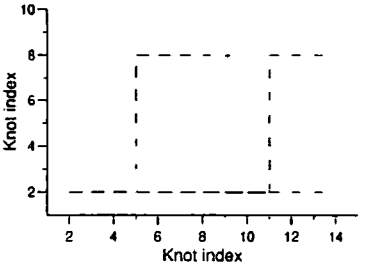

Figure 5: Result of the backtransformation. The size of the symbols correspond to the magnitude of the current in that direction. A standing wave is present in the upper left branch of the coupler and the Ports A,B and D are clearly visible.

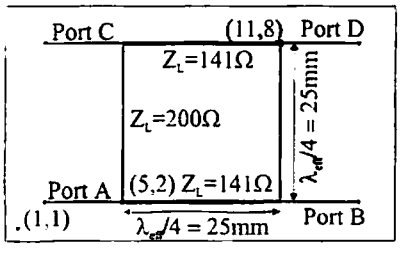

Figure 6: Branch line coupler on a RT-duroid substrate ($h = 0.79mm$, $\epsilon_r = 2.33$, $\tan\theta = 0.0012$), thin lines $Z_L = 200\Omega$ and Ports B-D terminated with $Z = 200\Omega$, $f = 2.25$GHz

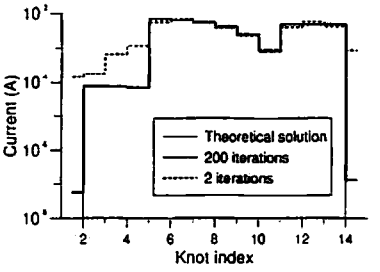

Figure 7: Current distribution along the upper conductor between Port C and D for different numbers of iterations.

6. Conclusion

An algorithm was developed for the efficient calculation of the current distribution on a printed circuit board from the measured electromagnetic fields above the board. This was accomplished by using Sommerfeld's theory for stratified media and the regularizing properties of the conjugate gradient method.

7. Acknowledgment

The authors would like to thank Daimler-Benz Aerospace Ulm and the German BMBF for supporting this contribution.

8. References

[1] G. Fässler, F. M. Landstorfer, and F. Wiedmann, *A Method to Investigate the Current Distribution on Printed Circuit Boards*, 11th International Zurich Symposium on Electromagnetic Compatibility, March 1995, pp. 459-464

[2] T. Itoh, *Numerical Techniques for Microwave and Millimeter-Wave Passive Structures*, John Wiley and Sons. New York, 1986, pp. 133-213

[3] J. R. Mosig and T. K. Sarkar, *Comparison of Quasi-Static and Exact Electromagnetic Fields from a Horizontal Electric Dipole above a Lossy Dielectric Backed by an Imperfect Ground Plane*, IEEE Transactions on Microwave Theory and Techniques, Vol. MTT-34, No. 4, April 1986

[4] P. C. Hansen, *Numerical Tools for Analysis and Solution of Fredholm Integral Equations of the First Kind*, Inverse Problems 8 (1992), pp. 849-872

[5] P. C. Hansen, *Analysis of Discrete Ill-Posed Problems by Means of the L-Curve*, SIAM Rev. 34 (1992), pp. 561-580